2496 *Inorg. Chem.* **2010**, *49*, 2496–2501
DOI: 10.1021/ic902401k

Inorganic Chemistry
Article

Effect of Electron-Withdrawing Dithiolate Bridge on the Electron-Transfer Steps in Diiron Molecules Related to $[2Fe]_H$ Subsite of the [FeFe]-Hydrogenases

Kévin Charreteur, Mohamed Kdider, Jean-François Capon, Frédéric Gloaguen,* François Y. Pétillon, Philippe Schollhammer,* and Jean Talarmin

Université Européenne de Bretagne; Université de Brest; CNRS UMR 6521 "Chimie, Electrochimie Moléculaires et Chimie Analytique"; ISSTB; CS 93837, 29238 Brest, France

Received December 4, 2009

Two hexacarbonyl diiron compounds featuring dithiolate bridges with strong electron-withdrawing groups (CO_2Me, tetrachloro-biphenyl) were synthesized and structurally characterized. Electrochemical study of these compounds demonstrates that such electron-withdrawing groups have a pronounced effect on both the reduction potentials and the electron transfer process. The reduced forms of these compounds catalyze the reduction of protons in dichloromethane. However, the tetrachloro-biphenyl derivative is the only one able to work in the potential range of its primary reduction process. A catalytic reaction scheme is proposed.

Introduction

Improvement of the efficiency of electrocatalysts based on a [2Fe2S] core, bioinspired by the active site of [FeFe]-hydrogenase (Scheme 1), for the reduction of protons to dihydrogen still requires an intensive and rationalized development of chemistry and electrochemistry of diiron dithiolate molecules.[1] The stereoelectronic control of the diiron site activity at the first or second coordination sphere level can be exerted through the choice of the ligands, which direct the primary step of the process toward either a protonation or reduction reaction.

Recent works were focused on the use of chelating ligands to induce the formation of a terminal hydride functionality at the first step of the process, aimed at improving the kinetic of the electrocatalysis.[2] The effect of a base, as a proton relay in the diiron coordination sphere, has been also investigated.[3] In parallel to these works, very detailed electrochemical studies of a series of hexacarbonyl dithiolate diiron complexes of general formula $[Fe_2(CO)_6(\mu\text{-dithiolate})]$, that cannot be readily protonated, have shown that the choice of the bridging dithiolate group and the strength of the acid have a

Scheme 1

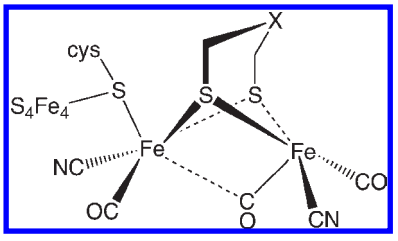

*To whom correspondence should be addressed. E-mails: fgloague@univ-brest.fr (F.G.), schollha@univ-brest.fr (P.S.).

(1) (a) Capon, J.-F.; Gloaguen, F.; Pétillon, F. Y.; Schollhammer, P.; Talarmin, J. *Coord. Chem. Rev*. **2009**, *253*, 1476–1494. (b) Tard, C.; Pickett, C. J. *Chem. Rev*. **2009**, *109*, 2245–2274. (c) Gloaguen, F.; Rauchfuss, T. B. *Chem. Soc. Rev*. **2009**, *38*, 100–108. (d) Felton, G. A. N.; Mebi, C. A.; Petro, B. J.; Vannucci, A. K.; Evans, D. H.; Glass, R. S.; Lichtenberger, D. L. *J. Organomet. Chem*. **2009**, *694*, 2681–2699. (e) Capon, J.-F.; Gloaguen, F.; Pétillon, F. Y.; Schollhammer, P.; Talarmin, J. *C. R. Chim*. **2008**, *11*, 842–851. (f) Capon, J.-F.; Gloaguen, F.; Pétillon, F. Y.; Schollhammer, P.; Talarmin, J. *Eur. J. Inorg. Chem*. **2008**, 4671–4681.

(2) (a) Orain, P.-Y.; Capon, J.-F.; Kervarec, N.; Gloaguen, F.; Pétillon, F.; Pichon, R.; Schollhammer, P.; Talarmin, J. *Dalton Trans*. **2007**, 3754–3756. (b) Morvan, D.; Capon, J.-F.; Gloaguen, F.; Le Goff, A.; Marchivie, M.; Michaud, F.; Schollhammer, P.; Talarmin, J.; Yaouanc, J.-J. *Organometallics* **2007**, *26*, 2042–2052. (c) Ezzaher, S.; Capon, J.-F.; Gloaguen, F.; Pétillon, F. Y.; Schollhammer, P.; Talarmin, J.; Pichon, R.; Kervarec, N. *Inorg. Chem*. **2007**, *46*, 3426–3428. (d) Adam, F. I.; Hogarth, G.; Kabir, S. E.; Richards, I. *C. R. Chim*. **2008**, *11*, 890–905. (e) Ezzaher, S.; Capon, J.-F.; Gloaguen, F.; Pétillon, F. Y.; Schollhammer, P.; Talarmin, J.; Pichon, R.; Kervarec, N. *C. R. Chim*. **2008**, *11*, 906–914. (f) Ezzaher, S.; Capon, J.-F.; Gloaguen, F.; Pétillon, F. Y.; Schollhammer, P.; Talarmin, J. *Inorg. Chem*. **2007**, *46*, 9863–9872. (g) Duan, L.; Wang, M.; Li, P.; Na, Y.; Wang, N.; Sun, L. *Dalton Trans*. **2007**, 1277–1283. (h) Barton, B. E.; Rauchfuss, T. B. *Inorg. Chem*. **2008**, *47*, 2261–2263. (i) Wang, N.; Wang, M.; Liu, T.; Zhang, T.; Darensbourg, M. Y.; Sun, L. *Inorg. Chem*. **2008**, *47*, 6948–6955. (j) Harb, M. K.; Windhager, J.; Daraosheh, A.; Görls, H.; Lockett, L. T.; Okumura, N.; Evans, D. H.; Glass, R. S.; Lichtenberger, D. L.; El-Khateeb, M.; Weigand, W. *Eur. J. Inorg. Chem*. **2009**, 3414–3420. (k) Morvan, D.; Capon, J.-F.; Gloaguen, F.; Pétillon, F.; Schollhammer, P.; Talarmin, J.; Yaouanc, J.-J; Michaud, F.; Kervarec, N. *J. Organomet. Chem*. **2009**, *694*, 2801–2807. (l) Ezzaher, S.; Capon, J.-F.; Dumontet, N.; Gloaguen, F.; Pétillon, F. Y.; Schollhammer, P.; Talarmin, J. *J. Electroanal. Chem*. **2009**, *626*, 161–170. (m) Zampella, G.; Fantucci, P.; De Gioia, L. *J. Am. Chem. Soc*. **2009**, *131*, 10909–10917. (n) Barton, B. E.; Zampella, G.; Justice, A. K.; De Gioia, L.; Rauchfuss, T. B.; Wilson, S. R. *Dalton Trans*. **2009**, DOI: 10.1039/b910147k.

(3) (a) Ezzaher, S.; Orain, P.-Y.; Capon, J.-F.; Gloaguen, F.; Pétillon, F. Y.; Roisnel, T.; Schollhammer, P.; Talarmin, J. *Chem. Commun*. **2008**, 2547–2549. (b) Ezzaher, S.; Capon, J.-F.; Gloaguen, F.; Pétillon, F. Y.; Schollhammer, P.; Talarmin, J.; Kervarec, N. *Inorg. Chem*. **2009**, *48*, 2–4. (c) Wang, N.; Wang, M.; Zhang, T.; Li, P.; Liu, J.; Sun, L. *Chem. Commun*. **2008**, 5800–5802.

 Published on Web 02/05/2010

strong influence on both the potentials of the electrocatalytic events and the intimate mechanism of the electron transfer.[4] It has recently been reported that some dithiolate bridges featuring electron-withdrawing groups such as *o*-carborane,[5] naphtalene,[6] or biphenyl[7] favor the transfer of two electrons at the bimetallic site via two sequential reversible one-electron steps. A similar electrochemical response was also observed in a diiron compound bearing a benzo-[*c*]-cinnoline bridge.[8] The first reduction step gives rise to a stabilized diiron Fe(I)−Fe(0) species, which is a key intermediate in the electrocatalytic process. Studies of such mixed-valence compounds, having various dithiolate bridges, should give new insights into the understanding of the electrocatalytic process of the proton reduction, as well as new guidelines for the elaboration of efficient diiron electrocatalysts that could be coupled with a photosensitizer.[9]

With this goal, we have pursued our exploration of the effect of bridging groups on the electron transfer processes and the proton reduction catalysis at a diiron site by studying complexes having electron-withdrawing tetrachlorobiphenyl dithiolate or dithiolene bridges.

Results and Discussion

Synthesis and Characterization of $[Fe_2(CO)_6(\mu$-dithiolate$)]$ [dithiolate = $S_2C_2(CO_2Me)_2$ (1), tetrachloro-biphenyl-2,2′-dithiolate (Cl_4bpdt) (2)]. Compounds **1**[10] and **2** were obtained by well-known procedures using complexes $[Fe_2(CO)_6(\mu\text{-}S_2)]$ and $[Fe_3(CO)_{12}]$ as precursors, respectively (Scheme 2). Spectrocopic data of **1** were similar to those reported in the literature.[10] The infrared spectrum, recorded in hexane displays several bands in the ν_{CO} region at 2085 (m), 2044 (s), 2008 (s), 1993 (m), 1967 (w), 1957(w), and 1723(w) cm^{-1}. The ^1H NMR spectrum of **1** in $CDCl_3$ exhibits one singlet at 3.72 ppm, assigned to two equivalent methyl groups of the dithiolate-bridge. The $^{13}C\text{-}\{^1H\}$ NMR spectrum in $CDCl_3$ shows four signals at 206.5, 162.2, 155.4, and 53.2 ppm that are attributed to the *C*≡O, CO_2, *C*=*C*, and CH_3 groups, respectively. The IR

Scheme 2

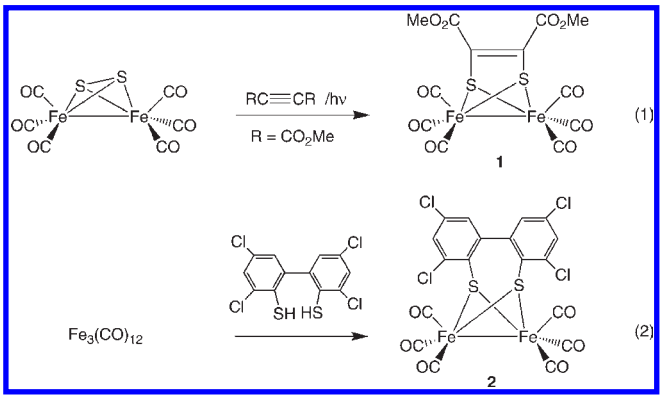

spectrum of compound **2** in hexane shows three strong bands in the carbonyl region (2082, 2050, 2014 cm^{-1}), which is typical of a dithiolato bridged diiron hexarbonyl compound. The ^1H NMR spectrum in $CDCl_3$ exhibits two signals at 7.00 and 7.53 ppm attributed to the aromatic protons of the tetrachlorobiphenyl group. X-ray analysis of single crystals of complex **1** and **2**, obtained respectively from diethyl ether and pentane solutions at −15 °C, established without any ambiguity their geometry and the nature of the bridging groups. (Figure 1 and Table 1). **1** and **2** are structurally analogous with other diiron(I) hexacarbonyl dithiolato-bridged species with two eclipsed $\{Fe(CO)_3\}$ groups bridged by a dithiolate ligand, the geometry around each iron atom being a distorted square pyramid supplemented by a Fe−Fe single bond. The torsion angle between the two phenyl rings is 46.3° in compound **2**. Other distances and angles are unexceptional (Table 1).

Electrochemical Behaviors of Compounds 1 and 2. The electrochemical properties of the diiron derivative were probed by cyclic voltammetry (CV). **1** was found unstable in MeCN/ and thf/Bu_4NPF_6. New redox peaks appears after a period of several minutes, but not in CH_2Cl_2/Bu_4NPF_6 electrolyte. A similar behavior was observed for $Fe_2(SCH_2C_6H_4CH_2S)(CO)_6$ in MeCN.[4b] A possible explanation is that a small amount of the reduced form of **1** generated by CV triggers an electron transfer catalyzed (ETC) substitution of CO for MeCN or thf in solution.[11] This process is not observed in CH_2Cl_2, which is a weaker donating solvent. In contrast, complex **2** was found to be stable in all electrolytes.

In CH_2Cl_2/Bu_4NPF_6, the primary reduction of **1** and **2** takes place at $E_{1/2}^{red1} = -1.11$ and −1.05 V, respectively, that is, at a potential about 0.7 V milder than for the reduction of the propanedithiolate derivative (Table 2). This result emphasizes the strong effect of the dithiolene and tetrachloro-biphenyl dithiolate groups on the level of the lowest unoccupied molecular orbital (LUMO). As shown in Figure 2, a second well-resolved reduction process occurs at a slightly more negative potential ($E_{1/2}^{red2} = -1.25$ and −1.40 V for **1** and **2**, respectively). The peak current (I_p^{red}) varies as the square root of the scan rate (v) for $0.02 \le v \le 2$ V s^{-1}, consistent with a diffusion-limited electron-transfer for both reduction steps (Figures S1 and S2 in the Supporting Information). It is difficult to extrapolate the number of electrons

(4) (a) Borg, S. J.; Berhsing, T.; Best, S. P.; Razavet, M.; Liu, X.; Pickett, C. J. *J. Am. Chem. Soc.* **2004**, *126*, 16988–16999. (b) Capon, J.-F.; Gloaguen, F.; Schollhammer, P.; Talarmin, J. *J. Electroanal. Chem.* **2004**, *566*, 241–247. (c) Capon, J.-F.; Gloaguen, F.; Schollhammer, P.; Talarmin, J. *J. Electroanal. Chem.* **2006**, *595*, 47–52. (d) Gloaguen, F.; Morvan, D.; Capon, J.-F.; Schollhammer, P.; Talarmin, J. *J. Electroanal. Chem.* **2007**, *603*, 15–20. (e) Capon, J.-F.; Ezzaher, S.; Gloaguen, F.; Pétillon, F. Y.; Schollhammer, P.; Talarmin, J.; Davin, T. J.; McGrady, J. E.; Muir, K. W. *New J. Chem.* **2007**, *31*, 2052–2064. (f) Felton, G. A. N.; Vannucci, A. K.; Chen, J.; Lockett, L. T.; Okumura, N.; Petro, B. J.; Zakai, U. I.; Evans, D. H.; Glass, R. S.; Lichtenberger, D. L. *J. Am. Chem. Soc.* **2007**, *129*, 12521–12530. (g) Capon, J.-F.; Ezzaher, S.; Gloaguen, F.; Pétillon, F. Y.; Schollhammer, P.; Talarmin, J. *Chem.—Eur. J.* **2008**, *14*, 1954–1964. (h) Borg, S. J.; Ibrahim, S. K.; Pickett, C. J.; Best, S. P. *C. R. Chim.* **2008**, *11*, 852–860. (i) Felton, G. A. N.; Petro, B. J.; Glass, R. S.; Lichtenberger, D. L.; Evans, D. H. *J. Am. Chem. Soc.* **2009**, *131*, 11290–11291.

(5) Schwartz, L.; Eriksson, L.; Lomoth, R.; Teixido, F.; Vinas, C.; Ott, S. *Dalton Trans.* **2008**, 2379–2381.

(6) Wright, R. J.; Lim, C.; Tilley, T. D. *Chem.—Eur. J.* **2009**, *15*, 8518–8525.

(7) Singh, P. S.; Rudbeck, H. C.; Huang, P.; Ezzaher, S.; Eriksson, L.; Stein, M.; Ott, S.; Lomoth, R. *Inorg. Chem.* **2009**, *48*, 10883–10885.

(8) Orain, P.-Y.; Capon, J.-F.; Gloaguen, F.; Schollhammer, P.; Talarmin, J. *Int. J. Hydrogen Energy* **2010**, accepted for publication.

(9) (a) Wang, M.; Na, Y.; Gorlov, M.; Sun, L. *Dalton Trans.* **2009**, 6458–6467. (b) Lomoth, R.; Ott, S. *Dalton Trans.* **2009**, 9952–9959. (c) Streich, D.; Astuti, Y.; Orlandi, M.; Schwartz, L.; Lomoth, R.; Hammarström, L.; Ott, S. *Chem.—Eur. J.* **2009**, *16*, 60–63.

(10) Seyferth, D.; Henderson, R. S. *J. Organomet. Chem.* **1979**, *182*, C39–C42.

(11) Morvan, D.; Capon, J.; Gloaguen, F.; Schollhammer, P.; Talarmin, J. *Eur. J. Inorg. Chem.* **2007**, 5062–5068.

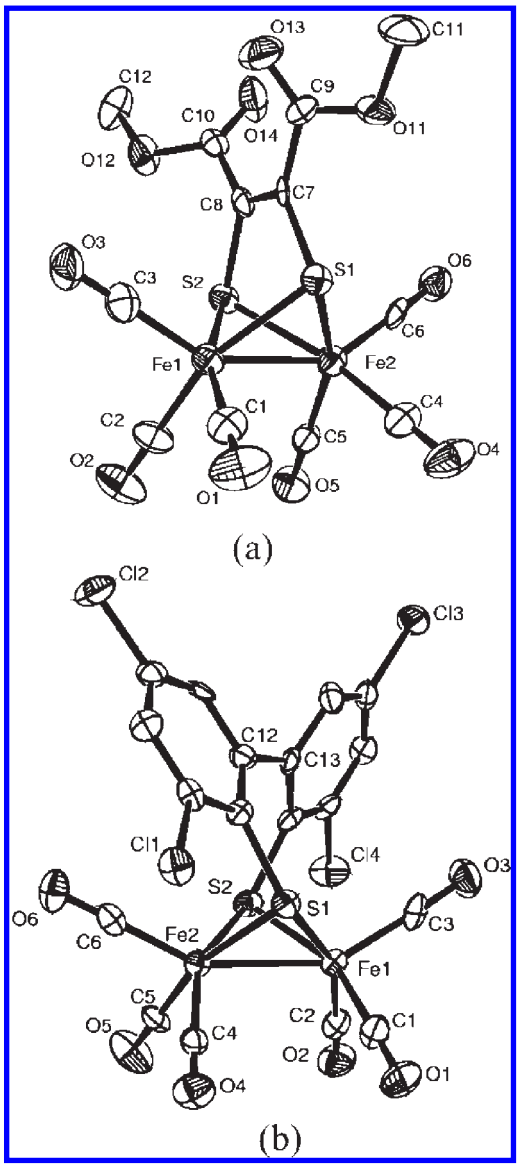

Figure 1. Molecular structures of $[Fe_2(CO)_6\{\mu\text{-}(SCCO_2Me)_2\}]$ (**1**) (a) and $[Fe_2(CO)_6(\mu\text{-}Cl_4bpdt)]$ (**2**·CH_2Cl_2) (CH_2Cl_2 is omitted for clarity) (b) with thermal ellipsoids at 50% probability.

involved in the reduction events from the slope of the I_p^{red} versus $v^{1/2}$ plot because the diffusion coefficients of **1** and **2** might have a very different value. However, the transfer of one electron in the first reduction step of complex **2** was confirmed by bulk electrolysis.

CV of **1** indicates that the two reduction steps are chemically reversible ($I_{p,a}/I_{p,c} \sim 1$) even at fast scan rate (Figure 2(a), and Figure S3 in the Supporting Information). A similar voltammetric response was reported for $[Fe_2(CO)_6(\mu\text{-SRS})]$ with R = *o*-carborane[5] or biphenyl,[7] as well as for $[Fe_2(CO)_6(\mu\text{-NRN})]$ with NRN = benzo-[*c*]-cinnoline.[8] In contrast, the primary reduction process of **2** appears less straightforward, as suggested by the shape of the oxidation peak on the reverse scan (Figure 2(b)). CV at fast scan rate reveals that this peak is the convolution of two oxidation events (Figure S4 in the Supporting Information). This observation is at odds with the recent report by Ott and coworkers[7] who showed that the first reduction step of a diiron derivative bearing a non-chlorinated biphenyl

Table 1. Selected Bond Lengths (Å) and Angles (deg) for **1** and **2**

distances (Å) and angles (deg)	**1**	**2**
Fe1−Fe2	2.4870(19)	2.5124(15)
Fe1−S1	2.274(3)	2.289(2)
Fe1−S2	2.281(3)	2.263(2)
Fe2−S1	2.272(3)	2.254(2)
Fe2−S2	2.270(3)	2.284(2)
C8−C7	1.311(10)	
C12−C13		1.496(10)
C8−C10	1.508(11)	
C7−C9	1.513(12)	
C10−O12	1.315(10)	
C10−O14	1.162(10)	
C9−O13	1.170(9)	
C9−O11	1.342(10)	
Fe1−C1	1.793(10)	1.802(9)
Fe1−C2	1.803(10)	1.788(10)
Fe1−C3	1.806(10)	1.798(9)
Fe2−C4	1.799(10)	1.809(9)
Fe2−C5	1.811(10)	1.816(9)
Fe2−C6	1.799(10)	1. 780(9)
C1−O1	1.114(10)	1.139(9)
C2−O2	1.123(10)	1.139(9)
C3−O3	1.144(9)	1.148(9)
C4−O4	1.130(9)	1.129(9)
C5−O5	1.140(9)	1.123(9)
C6−O6	1.154(9)	1.150(8)
Fe2−S2−Fe1/Fe2−S1−Fe1	66.25(8)/66.33(8)	67.00(7)/67.23(7)
C8−C7−C9	124.2(8)	
C8−C7−S1	118.0(7)	
C9−C7−S1	117.8(7)	
C7−C8−C10	127.2(8)	
C7−C8−S2	115.6(7)	
C10−C8−S2	117.2(7)	

Table 2. Reduction Potentials (vs $Fc^{+/0}$) of Various $[Fe_2(CO)_6(\mu\text{-dithiolate})]$ Compounds in CH_2Cl_2/Bu_4NPF_6

compound[a]	$E_{1/2}^{red1}$ /V (ΔE_p /V)	$E_{1/2}^{red2}$ /V (ΔE_p /V)	reference
$[Fe_2(CO)_6(\mu\text{-pdt})]$	−1.74 (0.13)		this work
$[Fe_2(CO)_6(\mu\text{-bdt})]$	−1.44 (0.09)		4b
$[Fe_2(CO)_6(\mu\text{-cdt})]$	−0.88 (0.09)[b]	−1.08 (0.10)	5
$[Fe_2(CO)_6(\mu\text{-bpdt})]$	−1.09 (0.11)	−1.30 (0.09)	7
1	−1.11 (0.12)	−1.25 (0.13)	this work
2	−1.05 (0.14)	−1.40 (0.15)	this work

[a] pdt = 1,3-propanedithiolate, bdt = 1,2-benzenedithiolate, cdt = *o*-carboranedithiolate, bpdt = biphenyl-2,2′-dithiolate. [b] In $MeCN/Bu_4NPF_6$.

dithiolate bridge is rather reversible at moderate scan rate. Thus, the presence of chlorine substituents in the biphenyl ring seems to affect the kinetics of charge transfer and the structure of the one-electron reduction product (vide infra).

Proton Reduction Catalysis with Complexes 1 and 2. As outlined by Evans and co-workers,[12] the lowest potential at which an acid can be reduced to hydrogen depends on the pK_a of this acid in the solvent being used. It is now well-established that, except in the case of azadithiolate derivatives, proton reduction by all-CO diiron compounds is initiated by a reduction step.[1,4] Since compounds **1** and **2** are reduced at very mild potentials, the proton reduction catalysis was first investigated using strong acids such as $HBF_4\cdot OEt_2$ or CF_3SO_3H ($pK_a \sim 3$ in MeCN).

Addition of $HBF_4\cdot OEt_2$ to a solution of **1** in CH_2Cl_2/Bu_4NPF_6 triggers the appearance of two new reduction events noted as waves (I) and (II) in Figure 3(a). At low

(12) Felton, G. A. N.; Glass, R. S.; Lichtenberger, D. L.; Evans, D. L. *Inorg. Chem.* **2006**, *45*, 9181–9184.

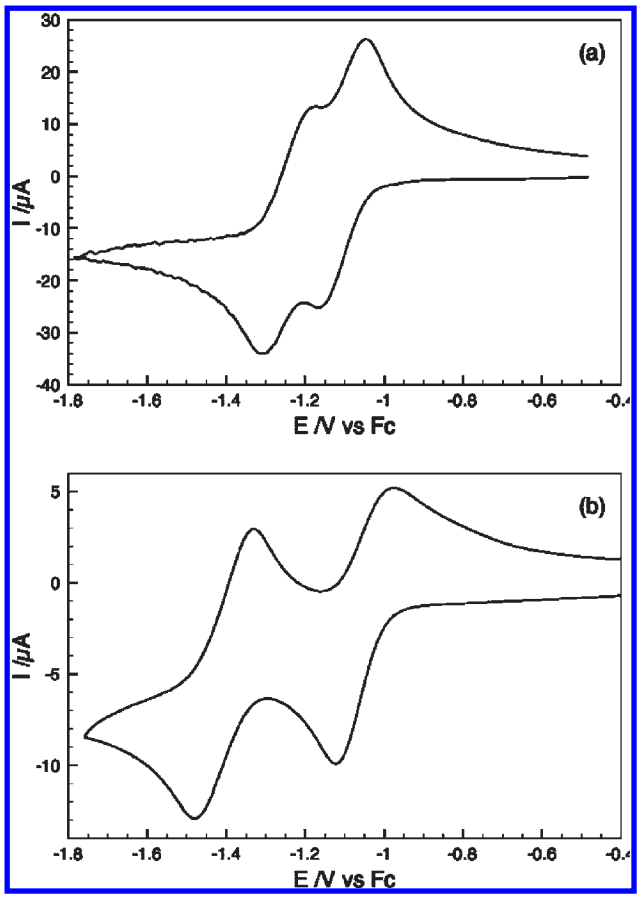

Figure 2. Voltammograms at 0.1 V s^{-1} in N_2-purged CH_2Cl_2/Bu_4NPF_6 of **1** (1.2 mM (a)) and **2** (0.6 mM (b)).

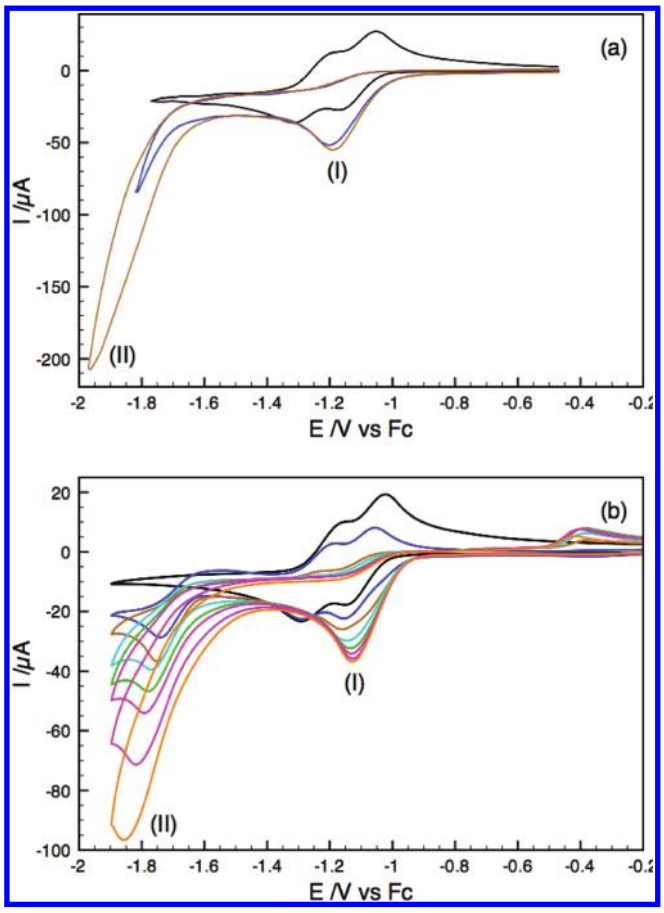

Figure 3. Voltammograms at 0.1 V s^{-1} in N_2-purged CH_2Cl_2/Bu_4NPF_6 of **1** + x equiv $HBF_4 \cdot OEt_2$: x = 0, 3, and 6 (a) and **1** + x equiv CCl_3CO_2H: x = 0, 1, 2, 3, 4, 5, 7, and 10 (b). Same conditions as in Figure 2.

acid concentration, wave (I) occurs at the same potential as that for the primary reduction of **1** and increases rapidly until it reaches a height that is about twice that of the $\mathbf{1}/\mathbf{1}^-$ reduction wave in absence of acid. These observations are consistent with an ECE mechanism in which the chemical step is the fast protonation of $\mathbf{1}^-$ by $HBF_4 \cdot OEt_2$. The subsequent protonation of the $2e^- + H^+$ species, **1**-H^-, is either kinetically slow or thermodynamically hindered, since a second reduction process noted as wave (II) occurs at $E < -1.75$ V, a potential significantly more negative than that of the $\mathbf{1}^-/\mathbf{1}^{2-}$ couple. Wave (II) is responsive to acid concentration and corresponds most certainly to the catalytic reduction of protons upon reduction of **1**-H^- to **1**-H^{2-}. Note, however, that at this potential the contribution of the reduction of the free protons may no more be negligible (see Figure S5 in the Supporting Information). To confirm the proposed catalytic mechanism (Scheme 3), CVs of **1** were recorded in the presence of a CCl_3CO_2H ($pK_a \sim 10$ in MeCN) (Figure 3(b)), which is a significantly weaker acid than $HBF_4 \cdot OEt_2$. As previously observed, the addition of acid triggers the occurrence of two new reduction events. Wave (I) shifts negatively and increases with acid concentration until it reaches a height that is again about twice that of the $\mathbf{1}/\mathbf{1}^-$ reduction wave in absence of acid, while wave (II) at -1.75 V continues to grow in height confirming its catalytic character. Note also the presence of an oxidation event at -0.45 V, ascribed to the oxidation of **1**-H^- to **1**-H, which confirms the formation of a stable $2e^- + H^+$ intermediate species.

Scheme 3. A = Compound **1** or **2**

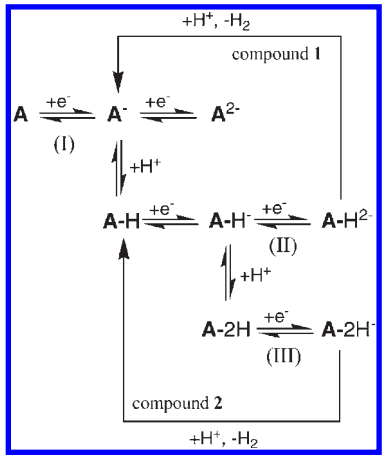

Addition of CF_3SO_3H (or $HBF_4 \cdot OEt_2$) to a solution of **2** in CH_2Cl_2/Bu_4NPF_6 triggers the appearance of a catalytic wave at about -1.3 V noted as wave (III) in Figure 4. At low acid concentration, wave (III) occurs at a potential slightly less negative than the $\mathbf{2}^-/\mathbf{2}^{2-}$ couple. There are also two additional waves noted as waves (I) and (II). Waves (I) and (II) do not increase significantly in height as the acid concentration becomes greater than 3 molar equiv. By analogy with the voltammetric behavior of complex **1**, wave (I) corresponds hence to an ECE process leading to **2**-H^-. Since $\mathbf{2}^-$ protonates in the presence of

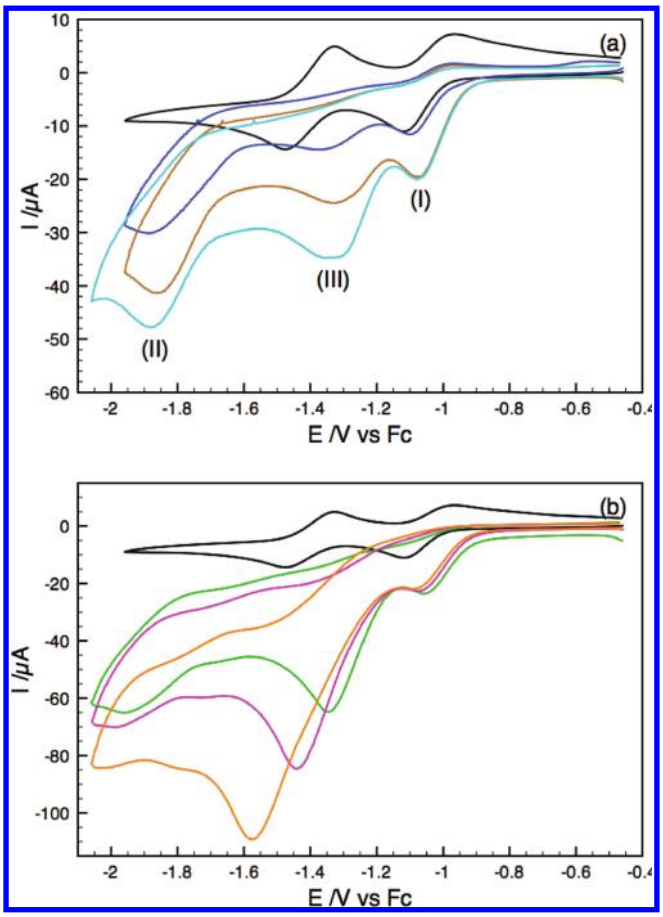

Figure 4. Voltammograms at 0.1 V s^{-1} in N_2-purged CH_2Cl_2/Bu_4NPF_6 of **2** + *x* equiv. CF_3SO_3H: $x = 0$, 1.3, 2.6, 3.9 (a) and $x = 0$, 6.5, 9.1, 13.0 (b). Same conditions as in Figure 2.

acid, catalytic wave (III) cannot be related to the $\mathbf{2}^-/\mathbf{2}^{2-}$ couple. We postulate that the wave (III) corresponds to the reduction of **2**-2H formed upon protonation of **2**-H^-. The overall catalytic process involves hence the formation of **2**-2H at the potential of the $\mathbf{2}/\mathbf{2}^-$ couple, the reduction of **2**-2H to **2**-$2H^-$ at about −1.3 V, and finally the protonation of **2**-$2H^-$ producing H_2 and regenerating **2**-H^- (Scheme 3). The detection of the reduction of **2**-H^- (wave (II)) at low acid concentration provides further support for the proposed mechanism. In the presence of a weaker acid such as CCl_3CO_2H, wave (III) is not observed and catalysis occurs at the potential of wave (II), as for compound **1**.

CVs in the presence of acid indicate that proton reduction catalysis by **2** is weak. Hydrogen evolution was nevertheless confirmed by bulk electrolysis experiments. Electrolysis at −1.45 V of a solution of **2** and 25 molar equiv of $HBF_4 \cdot OEt_2$ produced about 0.1 mL of H_2 over a period of 10 min (see Experimental Section). About 8 mols of electrons per mole of **2** (TON ∼ 4) were consumed in 2 h. The CV and IR spectrum recorded after the electrolysis showed no significant degradation of the starting compound.

Conclusion

The present study demonstrates that dithiolate bridges featuring electron-withdrawing groups have a pronounced effect on both the reduction potentials and the electron transfer process. This result is of particular interest in the perspective of coupling of the diiron hydrogenase mimics to light harvesting chromophores, since each absorbed photon leads to charge separation on the single electron level.[9]

As expected, the reduced forms of compounds **1** and **2** are both able to catalyze the reduction of protons. Reduction of **1** in the presence of acid leads to the stable $2e^- + H^+$ species **1**-H^-, which cannot be further protonated on the voltammetric time scale even with strong acid ($pK_a \sim 3$). As a result 1-H^- has to be reduced at a rather negative potential to generate **1**-H^{2-}, which is basic enough to catalyze the reduction of weak acid ($pK_a > 10$). In contrast, the $2e^- + H^+$ species **2**-H^- reacts with strong acid to form **2**-2H, which is reduced at a potential less negative than the $\mathbf{2}^-/\mathbf{2}^{2-}$ couple. Reduction of **2**-2H in the presence of excess acid catalyzes the proton reduction at the relatively mild potential of −1.3 V (the pK_a value of CF_3SO_3H in MeCN leads to estimated that the activation overpotential is of the order of −1 V). This is a rare example of all-CO diiron complex featuring an electron withdrawing group and able to catalyze the proton reduction at a potential close to that of the first electron-transfer process. At present, we do not have any information on the possible structure of $\mathbf{2}^-$ and **2**-2H. However, complexes bearing an electron-withdrawing dithiolate bridge, such as **2**, were shown to form rather stable reduced species. Further work will focus on determining the possible protonation sites in $\mathbf{2}^-$ and **2**-H^-. Finally, it is hoped that use of functionalized biphenyl dithiolate ligands may provide greater activity for the catalysts.

Table 3. Crystallographic Data for Complexes **1** and **2**

	1	**2**
empirical formula	$C_{12}H_6Fe_2O_{10}S_2$	$C_{37}H_{10}Cl_{10}Fe_4O_{12}S_4$
formula weight	485.99	1352.59
temperature/K	170(2)	170(2)
crystal system	triclinic	orthorhombic
space group	$P\bar{1}$	*Pbcn*
a(Å)	8.0399 (6)	21.900(2)
b(Å)	19.2280(14)	12.0018(14)
c(Å)	24.781(2)	18.086(2)
α(deg)	106.673 (7)	
β(deg)	95.128(7)	
γ(deg)	100.072(6)	
V(Å^3)	3573.5(5)	4753.7(9)
Z	8	4
ρ_{calc}(Mg mm^{-3})	1.807	1.890
μ (mm^{-1})	1.905	1.993
crystal size (mm)	0.10 × 0.07 × 0.04	0.12 × 0.05 × 0.01
range of θ (deg)	3.07−25.35	2.76−24.71
reflections measured	25670	30063
R_{int}	0.1244	0.2128
unique data/parameters	13078/945	4052/303
R_1 [$I > 2\sigma(I)$]	0.0643	0.0633
R_1 (all data)	0.2022	0.1551
wR_2 (all data)	0.1021	0.1089
goodness of-fit on F^2	0.787	0.869
$\Delta\rho_{max}$, $\Delta\rho_{min}$/e Å^{-3}	0.517, −0.469	0.713, −0.445

Experimental Section

Methods and Materials. All the experiments were carried out under an inert atmosphere, using Schlenk techniques. $[Fe_2(CO)_6(\mu\text{-}S_2)]$,[13] $[Fe_2(CO)_6\{\mu\text{-}(SCCO_2CH_3)_2\}]$,[10] and 2,2′-dithio-3,3′,5,5′-tetrachlorobiphenyl (Cl_4bpdt)[14] were prepared

(13) Seyferth, D.; Henderson, R. S.; Song, L.-C. *Organometallics* **1982**, *1*, 125–133.
(14) (a) Ballman, J.; Fuchs, M. G. G.; Dechert, S.; John, M.; Meyer, F. *Inorg. Chem.* **2009**, *48*, 90–99. (b) Ballman, J.; Dechert, S.; Demeshko, S.; Meyer, F. *Eur. J. Inorg. Chem.* **2009**, 3219–3225. (c) Alexakis, A.; Polet, D.; Rosset, S.; March, S. *J. Org. Chem.* **2004**, *69*, 5660–5667.

according to reported procedures. The ^{1}H NMR spectra were recorded at room temperature in $CDCl_3$ solution with Bruker AMX 400 or AC300 spectrometers and were referenced to $SiMe_4$ (^{1}H). The infrared spectra were recorded on a Nicolet Nexus Fourier transform spectrometer. Chemical analyses were made by the Service de Microanalyses I.C.S.N., Gif sur Yvette, France or the Centre de Microanalyses du CNRS, Vernaison, France.

The electrochemical equipment consisted in either an Autolab PGSTAT12 driven by the GPES software or a PAR 273 driven by the M270 software. The cell and electrodes were as described previously.[4b,c] The working electrode was a glassy carbon disk 0.071 cm^2 in surface area. All the potentials (text, tables, and figures) are quoted against the ferrocene-ferrocenium couple; ferrocene was added as an internal standard at the end of the experiments. The volume of hydrogen produced upon electrolysis was measured as described by King et al.[15] In a typical experiment, electrolysis at −1.45 V of **2** (0.6 mM) + $HBF_4 \cdot OEt_2$ (25 mM) consumed 0.72 C in 10 min. Gas bubbles were clearly observed. The amount of water displaced in a graduated pipet leads to the estimate that about 0.1 mL of gas was evolved. Electrolysis at −1.45 V of a solution of $HBF_4 \cdot OEt_2$ without **2** did not produce any detectable amount of gas. Although not very precise, these experiments indicate that the Faraday's yield with **2** is close to 100%.

(15) King, D. M.; Bard, A. J. *Anal. Chem.* **1964**, *36*, 2351–2352.

(16) Programs used: (a) *SHELX97*; Sheldrick, G. M. University of Göttingen: Göttingen, Germany, 1998. (b) *WinGX - A Windows Program for Crystal Structure Analysis*; Farrugia, L. J. *J. Appl. Crystallogr.* **1999**, *32*, 837.

Crystal data (Table 3) for compounds **1** and **2** were collected on an Oxford Diffraction X-Calibur-2 CCD diffractometer, equipped with a jet cooler device and graphite-monochromated Mo−Kα radiation (λ = 0.71073 Å). The structures were solved and refined by standard procedures.[16]

Synthesis and Spectroscopic Data of [$Fe_2(CO)_6(\mu$-Cl_4bpdt)] (2). A mixture of 1 g (2.0 mmol) of [$Fe_3(CO)_{12}$] and 0.36 g (1 mmol) of 2,2′-dithio-3,3′,5,5′-tetrachlorobiphenyl (Cl_4bpdt) was warmed in toluene (150 mL) at 90 °C for 5 h, after which period of time the solution was evaporated to dryness under vacuum. The residue was then treated by chromatography, and **2** was separated from the starting material on a silica gel column. Complex **2** was eluted with hexane as a red band. After collection of this fraction and evaporation of hexane, **2** was obtained as a red powder (yield: 0.220 g, 35%). **2** was then recrystallized in pentane at −15 °C, giving small red needles.

IR (hexane, cm^{-1}): ν_{CO} 2082(s), 2050(s), 2014(s). ^{1}H NMR ($CDCl_3$, 25 °C): δ 7.53 (d, J = 2.4 Hz, 2H), 7.00 (d, J = 2.4 Hz, 2H) ppm. Anal. Calcd (%) for $C_{18}H_4Cl_4Fe_2O_6S_2$: C, 34.11; H, 0.64. Found: C, 34.23; H, 0.58.

Acknowledgment. The authors thank the CNRS, the ANR "CatH2", UBO for financial support and Dr François Michaud for recording the X-ray data. K.C. thanks la Région Bretagne "Programme CREATE" for funding.

Supporting Information Available: CIF files and additional voltammetric data. This material is available free of charge via the Internet at http://pubs.acs.org.